Modeling of Transition and Surface Roughness Effects in Boundary-Layer Flows

W. J. Feiereisen* and M. Acharya†
Brown Boveri Research Center, Baden, Switzerland

Experiments were carried out to examine the influence of three-dimensional, stochastic roughness on the growth of incompressible turbulent boundary layers, as well as the effect of streamwise pressure gradients and freestream turbulence intensity on smooth-wall boundary-layer transition. The modeling of these effects in a two-dimensional boundary-layer computation program was examined with the help of the experiments. A model for surface roughness was developed that relates directly measurable statistical parameters quantifying the roughness geometry to the aerodynamic effects. This model should be valid for a limited class of surfaces found on turbomachinery blading and in other engineering applications. The transition comparisons point to shortcomings in models that are widely used to predict such flows. Commonly used criteria for the transition onset performed poorly and presumably need to be modified to account for other factors influencing the process. Additionally, models of the transition region should reflect intermittency variations through the boundary layer in the transverse direction and need to be modified to account for the rather strong effects of pressure gradient.

Nomenclature

A^+ = van Driest damping constant
c_f = skin-friction coefficient, $2\tau_s/\rho U_\infty^2$
C = empirical value in transition correlation
E_0 = constant in logarithmic law for mean velocity
F = roughness term in mixing length model
G = spot formation rate
k = roughness length scale
k_s = equivalent sand grain roughness scale
k^+ = roughness height in wall variables, ku_τ/v
ℓ = mixing length
ℓ^+ = mixing length in wall variables, $\ell u_\tau/v$
L_γ = extent of transition region between 25 and 75% intermittency points
M = freestream Mach number
R_a = centerline average roughness height
$Re_{L\gamma}$ = Reynolds number based on L_γ
Re_{tr} = transition Reynolds number based on x_{tr}
$Re_{\Delta x}$ = Reynolds number based on Δx
T_u = freestream turbulence intensity
u = velocity
Δu = velocity profile shift
u_∞ = freestream velocity
u_τ = shear velocity, $\sqrt{\tau_s/\rho}$
u^+ = velocity in wall variables, u/u_τ
x = streamwise coordinate
Δx = total extent of transition region
x_c = empirical value in roughness correlation
x_{tr} = location of transition onset relative to boundary-layer origin
y = transverse coordinate
y^+ = transverse coordinate in wall variables, yu_τ/v
α = empirical value in roughness correlation
$\langle\alpha\rangle$ = rms deviation of surface slope angles
β = empirical constant in roughness correlation
γ_{tr} = transition intermittency factor
δ = boundary-layer thickness
δ^* = boundary-layer displacement thickness
θ = boundary-layer momentum thickness
κ = von Kármán constant
λ = correlation length
μ_t^+ = nondimensional eddy viscosity, $\ell^{+2}(du^+/dy^+)$
ν = kinematic viscosity
ξ = nondimensional location in transition region, see Eq. (3)
ρ = fluid density
τ_s = wall shear stress

Introduction

THE operational characteristics and efficiency of turbomachines are strongly influenced by the boundary layers that develop on the blading surfaces. A major source of concern for designers is the inability to compute the development of these boundary layers with a sufficient degree of accuracy, stemming primarily from deficiencies in the modeling of laminar/turbulent transition and surface roughness effects. The present paper discusses some of the reasons for these deficiencies and suggests ways to improve the modeling of these effects in a boundary-layer computation procedure.

In the course of recent investigations at Brown Boveri, experiments were conducted to examine the influence of three-dimensional, stochastic roughness, of the type found on turbomachinery blading, on the growth of turbulent boundary layers, as well as the influence of freestream turbulence level and pressure gradients on the process of laminar/turbulent transition in the boundary layer on a hydraulically smooth surface. In addition to providing information to aid in the development of improved models of these processes, a number of fully documented data sets were obtained for use in comparisons with computations. In a parallel effort, a steady-state two-dimensional, finite-difference boundary-layer computation program was developed and modified to account for these effects. The present paper reports on some of the key features and results of the experiments and the boundary-layer computation program and compares the experimental results and calculations. Details of the experiments have been reported in Refs. 1 and 2.

Received Oct. 14, 1985; revision received Feb. 24, 1986.

*Research Scientist, Fluid Mechanics. Presently Scientist, Aerodynamics Division, NASA Ames Research Center, Moffett Field, CA.

†Research Scientist, Fluid Mechanics. Presently Visiting Associate Professor, Mechanical and Aerospace Engineering Department, Illinois Institute of Technology, Chicago, IL.

Background

Most calculation procedures for rough-wall boundary layers rely on a knowledge of the equivalent sand grain roughness k_s of a surface. A concept introduced by Schlichting,[3] it is a length scale defining the nominal sand grain size that would result in the same skin-friction coefficient as the surface under consideration at fully rough conditions. In principle, this concept allows one to make use of the results for sand grain roughness for any rough surface once the value of k_s/k is specified for that surface. However, the sand grain roughness length for a surface is an aerodynamic parameter and its relation to the readily measurable physical roughness remains unclear. Integral methods generally account for roughness through modified velocity profiles, together with skin-friction and Stanton number correlations based on the sand grain roughness Reynolds number. Differential methods such as that employed by Cebeci and Chang[4] use modified eddy viscosity formulations to account for surface roughness, again based on the equivalent sand grain roughness.

Experiments have shown that various roughness types have differing effects on boundary-layer development and that, for many roughness geometries, a single parameter representing the geometrical roughness is inadequate to specify the effect on skin friction. Parameters such as the roughness height, shape, density, and manner of distribution are important in determining the net effect of the roughness on the boundary layer. Betterman[5] and Dvorak[6] developed correlations relating the roughness function $\Delta u/u_\tau$, which represents the shift in the mean velocity profile due to the surface roughness, to a roughness height scale and a density parameter, while Dirling[7] attempted to relate the equivalent sand grain roughness of a surface to the height, density, and inclination of the roughness elements. These and other correlations have been extensively used in computational schemes for rough-wall boundary-layer flows with varying degrees of success. A large degree of uncertainty still exists in the use of correlations to determine the equivalent sand grain roughness for a general roughness geometry. Since it is an aerodynamic rather than a geometric quantity, an experiment is needed to establish k_s/k for each new surface considered. Alternative approaches to the problem (such as those of Lewis,[8] Finson,[9] and Lin and Bywater[10]), which avoid the concept of equivalent sand grain roughness altogether by modeling the skin-friction drag at a rough wall based on a consideration of the form drag on individual protruberences, also necessitate many simplifying assumptions and have not—as yet—proved usable for the treatment of rough surfaces in general.

A number of experimental investigations, including those of Turner,[11] Walker,[12] and Graziani et al.,[13] have shown that significant regions of the boundary layer over both compressor and turbine blading can be laminar or transitional. An accurate prediction of such boundary layers is essential to obtain reliable estimates of heat-transfer rates for the design of efficient blade-cooling systems. A number of factors combine to determine both the onset and length of the transition region; two important ones are the streamwise pressure gradient and the freestream turbulence level. The usual procedure is to account for these in terms of correlations such as those developed by Seyb[14] and Dunham,[15] which specify a critical transition Reynolds number as a function of these two factors. Efforts to compute such boundary layers (e.g., McDonald and Fish[16] and Forest[17]) have shown that models of the transition process are not adequate and point to a need for more experimental data that might provide guidelines for improving these models. A few investigations along these lines have been reported recently (i.e., those of Abu-Ghannam and Shaw[18] and Blair[19]).

Experiments

Wind Tunnel and Instrumentation

The wind tunnel and instrumentation have been described in detail by Acharya et al.[1] Measurements were made within the incompressible boundary layer developing on the upper wall of the working section. A boundary layer that was either laminar or turbulent from the leading edge could be obtained. The freestream turbulence level could be varied between 0.2 and 5% through the use of static grids. With the exception of the floating elements for the measurement of the wall shear stress, all instrumentation used was standard. Boundary-layer profile measurements were carried out using hot wires. Separate floating-element instruments were used for wall shear stress measurements for each of the surfaces tested. The design and operation of the floating elements have been described in detail by Acharya et al.[20] Data acquisition was accomplished using a custom-built system under the control of a PDP 11/04 minicomputer.

Surface Roughness Experiments

In the present approach to the problem, an effort was made to relate statistical descriptors of the roughness characteristics of surfaces to their effect on the boundary-layer skin friction. Surface microgeometry measurements were made on a series of turbomachinery blades manufactured and finished by a variety of processes. These measurements were used to identify the parameters (and their ranges) necessary for a statistical description of such surfaces: the centerline arithmetic average roughness R_a, the rms deviation of surface slope angles $\langle\alpha\rangle$, and a correlation length λ, defined as the distance at which the autocorrelation function of the vertical displacement falls to a value of 0.1. Boundary-layer measurements were carried out on four rough surfaces: 1) a surface with statistical properties based upon the measurements just described and representative of a wide class of turbomachinery

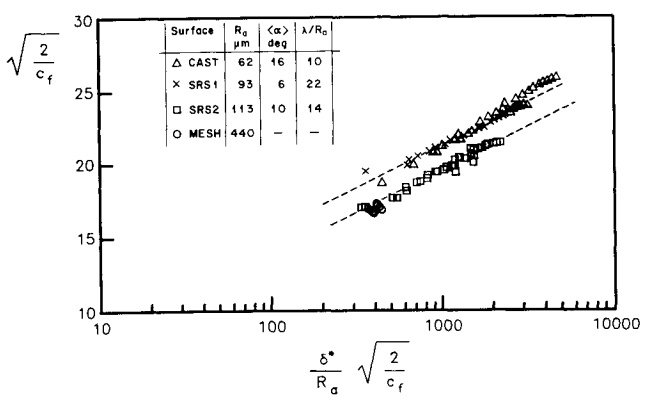

Fig. 1 Skin-friction correlation.

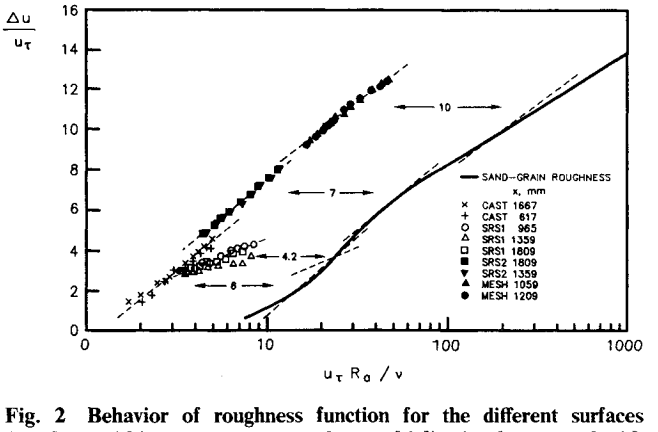

Fig. 2 Behavior of roughness function for the different surfaces (numbers within arrows correspond to multiplicative factor used with R_a to bring data into line with sand grain results).

blading, but scaled up for wind tunnel testing (designated SRS1); 2) a variant of this surface with different roughness parameters (designated SRS2); 3) a sand-cast surface; and 4) a mesh surface with a deterministic roughness geometry. Measurements were also carried out on a smooth surface to serve as a reference. A zero-pressure gradient was established in each case, with a nominal freestream velocity of 18.8 m/s. Data included measurements of the wall shear stress and profiles of the mean velocity and turbulence intensities through the boundary layer at a number of streamwise locations. The roughness function was obtained from a fitting procedure using the measured mean velocity profile and wall shear stress. The reader is referred to Ref. 1 for details. Wall shear stress data did not collapse completely when scaled with R_a (Fig. 1), indicating that this is not the only parameter to use in describing the effects of roughness on boundary layers. The roughness function plot (Fig. 2) showed that for a limited class of technically interesting rough surfaces represented by the surface SRS1 the value of k_s/R_a is about 4.2, whereas for the other scaled-up surface SRS2 the value is about 7. The rms deviation in slope angle seems to play an important role. Trends in the data indicate that k_s/R_a increases with $\langle\alpha\rangle$. However, additional measurements are needed with surfaces for which $\langle\alpha\rangle$ is systematically varied to obtain reliable relationships between $\langle\alpha\rangle$ and the aerodynamic parameters.

Boundary-Layer Transition Experiments

Three separate smooth-surface boundary layers were documented in detail to serve as test cases for comparison with the computed results. The first, designated TRA, was a baseline flow with zero streamwise pressure gradient, a freestream velocity of 18.8 m/s, and a freestream turbulence level of about 0.7%. The second boundary layer, TRB, was set up with the same approach velocity and external turbulence level as TRA, but with a strong streamwise acceleration followed by an adverse pressure gradient region such as might be found on a turbine blade. The third test boundary layer, TRC, was documented for the same pressure gradient distribution and approach velocity as TRB, but with a freestream turbulence level of 2.5%. The streamwise variation of the wall shear stress was measured using the floating element instrument. Also measured were the wall intermittency and profiles of the mean velocity, streamwise turbulence intensity, and intermittency factor at a number of boundary-layer locations in the laminar, transition, and turbulent regions. Figures 3 and 4 show the variation of near-wall intermittency and wall shear stress for the three test flows. Further details of these measurements and the additional experiments carried out to examine questions regarding the near-wall behavior of the mean velocity profile through the transition region, the asymptotic behavior of the

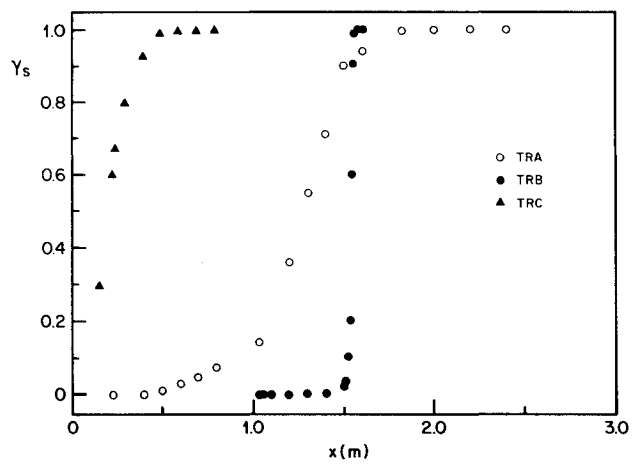

Fig. 3 Streamwise variation of wall intermittency, transition experiments.

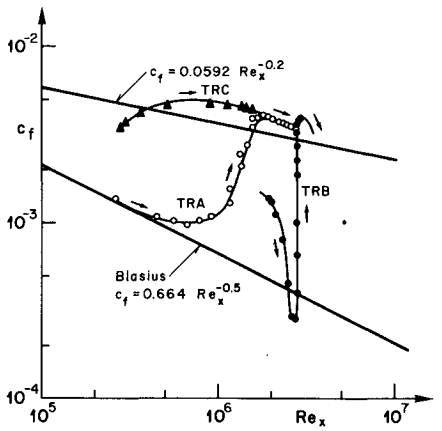

Fig. 4 Variation of skin friction, transition experiments (lines are best fits through data).

critical transitional Reynolds number with increasing freestream turbulence intensity T_u, and the combined effect of pressure gradient and T_u on the onset of transition have been described by Acharya.[2]

Computer Program Description

A main feature of the code, which is based on the Patankar-Spalding[21] method, is the use of so-called wall functions to implement the boundary conditions at the wall. These are semianalytical functions that relate the values of variables at the wall to those at the first finite-difference mesh point in the flow. The governing equations in the near-wall region can be reduced to ordinary differential equations and, following Crawford and Kays,[22] integrated numerically between the wall and the first mesh point. This approach eliminates the need to compute through regions of high gradients and results in a substantial reduction in the number of mesh points required and a consequent saving in CPU time. The same turbulence models are uniformly applied in both the wall function and finite-difference computation regions. The turbulence modeling is based on the work of Cebeci and Smith.[23]

The usual practice when simplifying the boundary-layer equations in the near-wall region is to neglect all streamwise derivatives apart from the pressure gradient term. However, it can be shown that retention of the latter when the corresponding convective terms have been neglected leads to mean velocity profiles that deviate widely from the accepted "log-law" behavior,‡ leading some researchers to the introduction of a "variable van Driest constant" to bring the velocity profile back into line with log law. In the present treatment, all derivatives in the streamwise direction were neglected in a consistent fashion and the resulting ordinary differential equations were numerically integrated from the wall to the first mesh point by use of a fourth-order Runge-Kutta method. The procedure followed by Crawford and Kays[22] was used to match to the finite-difference computation.

The Patankar-Spalding method involves a transformation into coordinates that expand with the boundary layer. This expansion is accomplished by means of "entrainment" or the introduction of mass through the edge of the computational mesh, to be distinguished from the physical entrainment at the edge of the boundary layer. Ideally, the entrainment is adjusted to keep the outer edge of the boundary layer within the computational mesh so that the external boundary conditions can be satisfied, while simultaneously ensuring that the extent of the freestream region covered by the mesh is kept to a minimum, thereby obtaining the maximum resolution over the

‡We acknowledge discussions with M.P. Escudier that brought this point to our attention.

boundary layer for a given mesh size. A proper control of this feature proved to be crucial in many calculations involving turbomachinery boundary layers. It was found that a damped algorithm based on the ratio of the total mesh height to the displacement thickness at the previous streamwise location yielded the most satisfactory results.

The numerical method employed is effectively a variation of the implicit Euler method, applied to the streamwise derivatives. The normal derivatives are eliminated by integrating the equations over control volumes around each mesh point, thus producing a set of coupled ordinary differential equations. The assumption of a step velocity profile between nodes proved to be adequate for this integration. The calculation begins with an initial velocity profile and proceeds downstream making the selection of a step size necessary at each forward step. Although the implicit method allows large step sizes, the explicit boundary conditions on the wall place a stability limit on the code. Three nondimensional numbers (obtained from a linear stability analysis and analogous to the well-known CFL condition or Courant number in time marching methods) are used at every step of the calculation to determine an optimal forward step size that accurately captures the spatial development with a minimum number of steps.

Surface Roughness Model

The principal effects of roughness are confined to the inner region of the boundary layer and characterized by the roughness function $\Delta u/u_\tau$. It is also generally accepted that the effects of roughness on the boundary layer are not coupled with those of the pressure gradient and thus may be modeled separately. The usual approach[4,16] has been to suitably modify the algebraic models of the mixing length (or eddy viscosity) in order to account for roughness. One of the goals of the present work was to build into such a model a direct connection between the directly measurable statistical quantities λ, R_a, and $\langle\alpha\rangle$ describing the surface roughness and their effect on the boundary-layer development. To achieve this, the mixing length is modified in a manner similar to the approach of Cebeci and Chang[4] as

$$\ell^+ = \kappa\left[y^+ + F\left(R_a^+, \langle\alpha\rangle\right)\right]\left(1 - e^{y^+/A^+}\right) \qquad (1)$$

The term F models the increased mixing length (and turbulent viscosity) in the inner region due to the roughness and is chosen to yield the required displacement of the mean velocity profile in the inner region coupled with a gradual fairing-in with the velocity profile in the outer region. To determine the appropriate form for F, data from the present experiments were used to obtain an interpolated tabulation of the equivalent sand grain size as a function of the variables R_a^+ and $\langle\alpha\rangle$. This tabulation was combined with the prescription suggested by Jayatilleke[24] for sand grain roughness,

$$0 < k^+ < 3.7 \quad \Delta u^+ = 0$$

$$3.7 < k^+ < 100 \quad \Delta u^+ = \frac{1}{\kappa}\ell n \frac{E_0}{\left[\alpha\left(k^+/\beta\right)^2 + (1-\alpha)E_{0-2}\right]^{\frac{1}{2}}}$$

$$k^+ > 100 \quad \Delta u^+ = \frac{1}{\kappa}\ell n\left(\frac{E_0 k^+}{\beta}\right) \qquad (2)$$

where β is an empirical constant with a value of 30.03, $\alpha = (1 + 2x_c^3 - 3x_c^2)$, $x_c = 0.002248\ (100 - k^+)/k^{+0.584}$, and E_0 is related to the additive constant B in the log law by $B = (1/\kappa)\ell n E_0$.

The Couette flow form of the boundary-layer equations was integrated using Eq. (1) for different values of the function F and the corresponding sand grain roughness Reynolds number was determined iteratively with the help of Eq. (2) to build a table of values of F as a function of the sand grain roughness

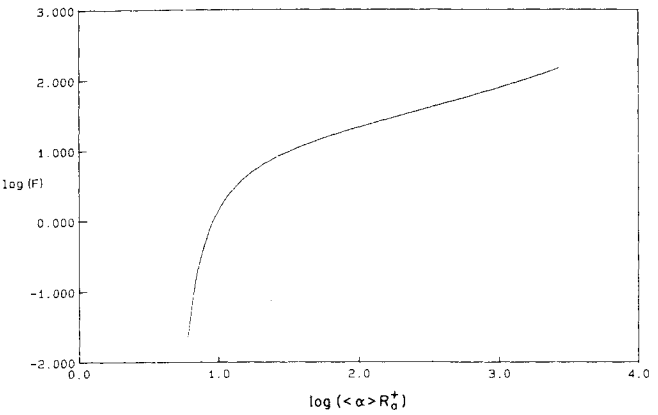

Fig. 5 Form of roughness function.

Reynolds number. With the help of the measurements the sand grain length was related to the measured geometric quantities and the functional form of F shown in Fig. 5 was fit to these values. We believe that the form of F should be valid for a fairly broad class of technically relevant roughness; however, it should be emphasized that this is drawn from a very limited set of measurements and further experiments are needed to establish a reliable relationship between the surface descriptors and aerodynamic parameters for general use in boundary-layer computations. The general approach as we have specified here would, however, remain valid.

The near-wall treatment results in velocity profiles that fair smoothly into the curve $u^+ = y^+$, implying some kind of universality near the wall. Although this is recognized as not generally being the case for rough walls, the procedure was used to provide a uniform way to model the displacement of the logarithmic portion of the mean velocity profile and, as will be seen later, yields good results for the integral quantities and skin friction.

Transition Model

To compute the development of transitioning boundary layers, the eddy viscosity model is empirically modified to account for the location of the start of transition and the length of the transition region. The critical momentum thickness Reynolds number Re_{tr} for the onset of transition is assumed to depend on the pressure gradient and freestream turbulence and is determined from one of the three correlations suggested by Seyb,[14] Dunham,[15] and Abu-Ghannam and Shaw.[18] Following Cebeci and Smith,[23] an intermittency function that permits the gradual introduction of turbulence into the boundary layer downstream of the transition onset point x_{tr} is used to modify the eddy viscosity. The length of the transition region depends on the form selected for this intermittency. The nondimensional momentum equation with the Couette flow assumptions becomes

$$\frac{du^+}{dy^+} = \frac{1}{1 + \gamma_{tr}\mu_t^+}$$

where γ_{tr} is the intermittency and μ_t^+ the eddy viscosity. With the definition of the mixing length [Eq. (1)], this can be rewritten as

$$\frac{du^+}{dy^+} = \frac{2}{1 + \left(1 + \gamma_{tr} 4\ell^{+2}\right)^{\frac{1}{2}}}$$

which is then integrated using the procedure described earlier. Cebeci and Smith suggest using the following correlation for the intermittency. This form was developed by Chen and Thyson[25] using the arguments of Emmons[26] and Dhawan and

Narasimha[27] that the intermittency distribution in the streamwise direction is Gaussian,

$$\gamma_{tr} = 1 - \exp\left[-G(x - x_{tr})\int_{x_{tr}}^{x} \frac{dx}{u_\infty}\right]$$

where G is a so-called spot formation rate parameter given by

$$G = (3/C^2)(u_\infty^3/\nu^2)\, Re_{tr}^{-1.34}$$

C is an empirical expression obtained by Chen and Thyson to relate the extent of the transition region to the Reynolds number at the start of transition and the Mach number M,

$$Re_{\Delta x} = C Re_{tr}^{\frac{2}{3}}$$

$$C = 60 + 4.86M^{1.92}, \qquad 0 < M < 5$$

The use of this and alternative approaches will be discussed later in connection with the comparisons with experimental results.

Computational Procedures

The measured velocity profile at the first streamwise location was used as a basis for constructing the initial conditions. A parameterized family of velocity profiles was fitted to the data using a least squares technique to provide a smooth starting profile. The finite difference grid was stretched in the nondimensional cross-stream coordinate such that the first point had a specified distance from the wall in wall coordinates and the ratio of the distance from the wall of the last point to the displacement thickness was approximately eight. This ratio was then maintained constant throughout the calculation.

Comparisons and Discussion

Rough-wall Boundary Layers

Calculations of the boundary-layer development over the two simulated rough surfaces, SRS1 and SRS2, were started using the measured profiles at the first streamwise location, $x = 0.159$ m, and carried through to the last measurement location, $x = 2.859$ m. The roughness function F for the two surfaces was determined as described earlier; the corresponding values for the equivalent sand grain roughness lengths were 0.390 and 0.791 mm, respectively.

Figure 6 shows the computed streamwise variation of the skin-friction coefficient for the two surfaces compared with the floating element measurements. The agreement is seen to be within the $\pm 5\%$ accuracy of the instrument. The corresponding comparisons for the variation of momentum thickness are shown in Fig. 7. The agreement is very good for SRS1 and quite reasonable for SRS2, in spite of small differences in slope. Figure 8 compares the computed and measured mean velocity profiles for SRS1 at $x = 2.859$ m, plotted in wall coordinates. In addition, the $u^+ = y^+$ curve and the smooth-wall "log law" are shown. The first finite-difference grid point is located at $y^+ = 20$. It can be seen that, while agreement is good in the logarithmic and other wake regions, the computations fair in to a sublayer region that is not representative of the measurements. This is an artifact of the way in which the roughness function has been handled in the near-wall region (measurements reflect the nonuniversality of the velocity in this region due to, for instance, the wakes of isolated roughness elements). The discrepancy does not, however, affect the results for c_f and the integral parameters and is, therefore, not serious as far as engineering calculations are concerned.

The roughness model used was developed with the help of experimental data obtained from SRS1 and SRS2; therefore, it is not surprising that the comparisons are good. It is argued that this model should be applicable for surfaces with statistically similar geometries, including a fairly large class of technically interesting surfaces. However, it is uncertain how far these results can be extrapolated; more experiments are needed in order to extend the correlation to a wider parameter range. The effects of roughness and compressibility on a turbulent boundary layer can be superposed, so that the present model could be used in the prediction of compressible flows as well.

Boundary-Layer Transition

Figure 9 shows the computed streamwise variations of c_f for flow TRA compared with the experimental data. It is seen that each of the three empirical criteria leads to a delayed prediction of the start of transition, while the computed length of the transition region is too short. This balancing effect results in a reasonable prediction for the end of the transition region. The corresponding predictions for the momentum thickness are shown in Fig. 10. The rate of increase of c_f in the central region is quite well predicted.

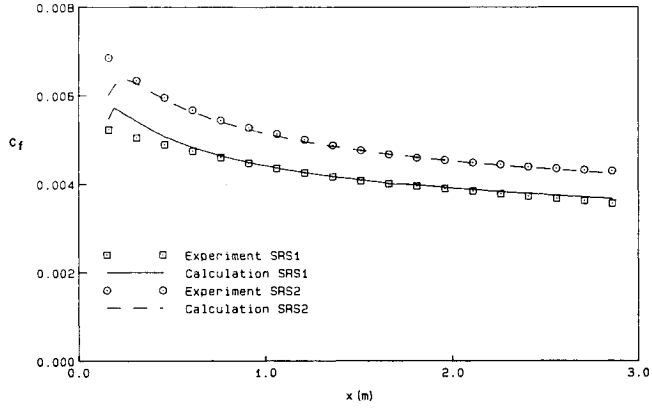

Fig. 6 Skin-friction comparisons, SRS 1 and SRS 2.

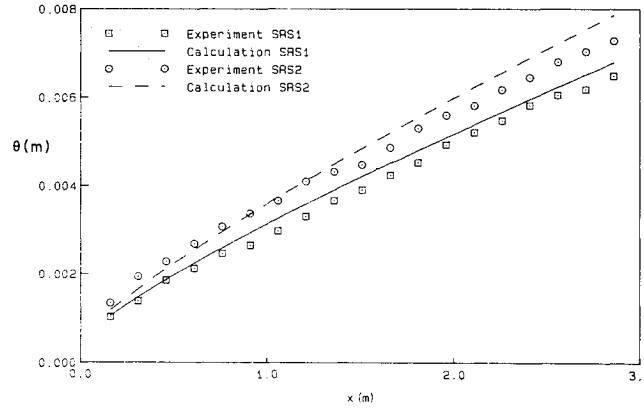

Fig. 7 Momentum thickness comparisons, SRS 1 and SRS 2.

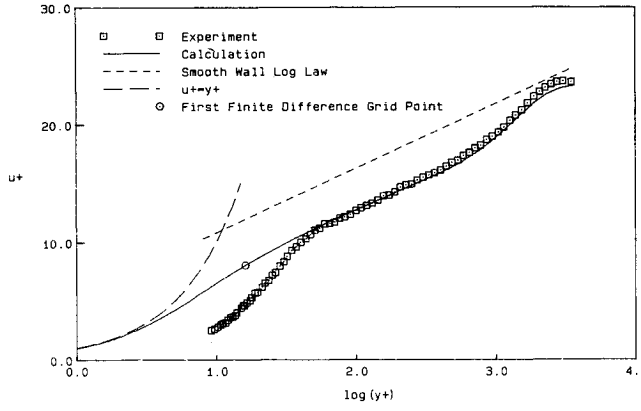

Fig. 8 Mean velocity profile comparisons, SRS 1, $x = 2.86$ m.

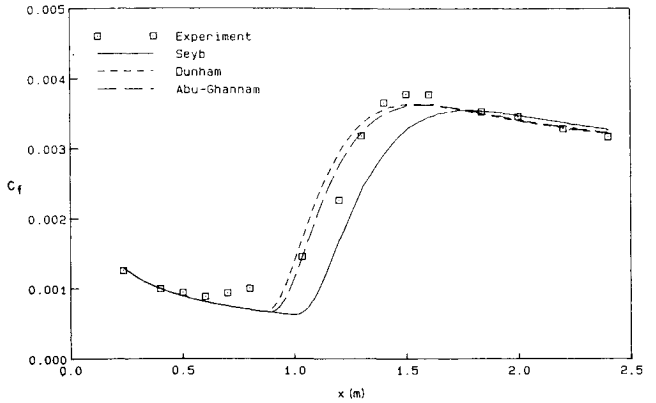

Fig. 9 Skin-friction comparisons, TRA.

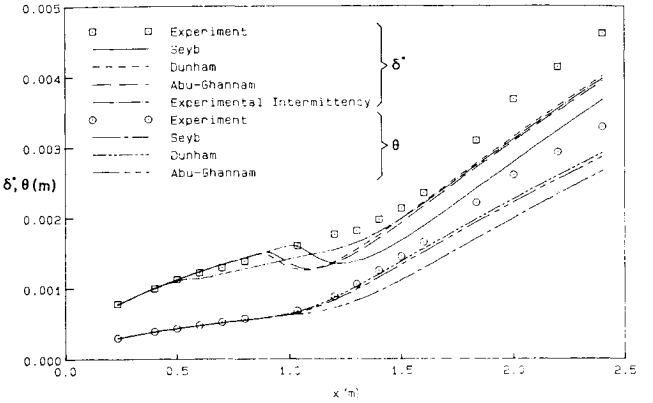

Fig. 10 Momentum and displacement thickness comparisons, TRA.

As this is a steady, zero pressure gradient smooth-surface flow, the only parameter that determines the onset of transition in the calculation is the freestream turbulence intensity. This was fixed in the calculation at the experimentally measured value; varying it over a range beyond the limits of experimental uncertainty did not account for the late prediction. One feature of transition that none of the correlations incorporate is the so-called unit Reynolds number effect discussed by Morkovin.[28] He points out that, under certain circumstances, the location of the onset of transition cannot be reliably predicted by the critical Reynolds number determined in the standard way because all of the various factors affecting the transition do not scale uniformly with the freestream velocity and fluid viscosity. Measurements by Acharya[2] have shown that at lower freestream turbulence intensities, where the influence of other factors is more likely to be important, the critical transition Reynolds number changes with the freestream velocity, although the turbulence intensity in the freestream is constant and a zero streamwise pressure gradient is maintained. Thus, other factors (for example, vibration or acoustic disturbances) that could play an important role in determining the onset of transition are not taken into account in these correlations.

In the modeling of transition, the critical Reynolds number criterion defines a location upstream of which the intermittency factor is zero and from which point onward the transition to turbulence sets in. In an actual boundary layer, this is not a well-defined point. Various definitions have been used by experimentalists in the past: the origin of the turbulent boundary layer obtained by extrapolating the boundary-layer thickness backward to a zero thickness, the point of minimum skin friction, the point where the near-wall intermittency reaches a prescribed value, the location where the velocity is a minimum on a streamwise traverse at a fixed height above the wall, etc. Application of these various criteria to the TRA flow resulted in a fairly wide spread: the minimum skin-friction location was around 600 mm, extrapolation of the turbulent boundary-layer thickness back to its origin yielded a value of 750 mm; the 1% intermittency location was at 500 mm; and the 5% intermittency point was at 750 mm. For such flows, where the wall intermittency rises very slowly in the beginning, the streamwise separation between the 1 and 5% intermittency points can be large; in this instance, it was 250 mm. In the calculations for this flow (see Fig. 9), the transition point specified by all three criteria was well beyond this region —at or after the location where the measured intermittency was 10%. The development of turbulence already has a significant effect on the flow at this location. Thus, it appears that these criteria cannot be used with complete reliability for this simplest kind of flow.

The second crucial aspect of the model is to determine the length of the transition region. As explained earlier, this is done through an intermittency distribution. Initial calculations using the Chen-Thyson[25] correlation showed that the computed intermittency rose far too quickly at the start of transition and that, consequently, the predicted length of the transition region was far too small. The likely reason is the spot formation rate; the value of the nondimensional rate $G\nu^2/u_e^3$ estimated from the experimental intermittency distribution (ignoring the non-Gaussian region described below) was found to be $2.13 \cdot 10^{-12}$, about one order of magnitude smaller than the value of $2.82 \cdot 10^{-11}$ obtained from the Chen-Thyson correlation. The experimentally determined distribution of intermittency shows reasonable agreement with the correlation,

$$\gamma(x) = 1 - \exp(-0.412\xi^2) \qquad \xi = (x - x_{tr})/L_\gamma \quad (3)$$

where

$$L_\gamma = x_{\gamma=0.75} - x_{\gamma=0.25}$$

suggested by Dhawan and Narasimha,[27] except for small deviations in the region close to the beginning of transition, suggesting departures from Gaussian behaviour in this region. As an alternative to the Chen-Thyson expression, the correlation

$$Re_{L_\gamma} = 5.0 Re_{tr}^{0.8}$$

suggested by Dhawan and Narasimha as being an appropriate relationship for low-speed flows was investigated. The spot formation rate deduced using this correlation compared very well with the experimental value.

All calculations shown were obtained using the Dhawan-Narasimha correlation. They represent an improvement over the results obtained using the Chen-Thyson correlation; one sees, however, that the prediction through the end of the transition region is still not very good. An examination of the computed displacement thickness in Fig. 10 shows that the use of an empirical intermittency distribution produces a marked dip at the beginning of the transition region and that the predicted values downstream are too low. When the experimentally determined near-wall intermittency distribution was used instead, a considerable improvement was obtained in the initial region, but discrepancies still remained over the second half of the transition region. A possible explanation for this shortcoming is the incorrect representation of the intermittency distribution in the transverse direction. The use of a scalar intermittency factor to weight the eddy viscosity formulation through transition implies that the transverse variation of eddy viscosity through the boundary layer is similar to that in a fully turbulent boundary layer. However, there is no

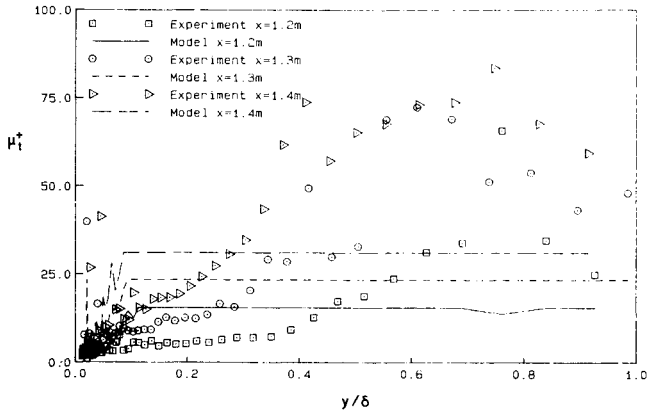

Fig. 11 Eddy viscosity distributions, TRA.

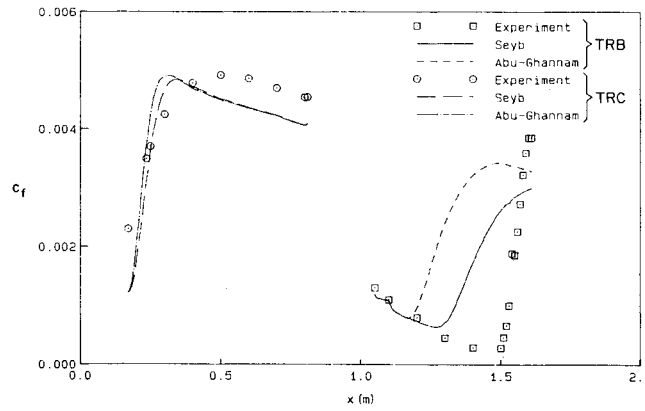

Fig. 12 Skin-friction comparisons, TRB and TRC.

reason to expect that the dynamics of a boundary layer undergoing transition are similar to that of a turbulent boundary layer; estimates of the transverse eddy viscosity distribution obtained from the experimental profiles at different streamwise locations through transition for the TRA flow showed that this is far from true. Figure 11 shows a comparison of these experimental estimates with the distributions used in the computation at three different locations in the transition region. It is seen that the eddy viscosity is overestimated in the inner region and underestimated in the outer part of the boundary layer where, in addition, the experiment indicates that the value is not constant but varies throughout the layer, increasing toward the outer edge. The crossover point also varies through the transition region. It must be concluded that a modeling of this behavior is necessary for a more accurate prediction of the boundary-layer growth through the transition region and beyond.

All three of the effects described above, the onset of transition, the extent of the region, and the transverse variation of intermittency, must be properly represented in the transition model in order to obtain a good prediction, since one factor affects the other. For instance, a late prediction of the transition onset is not compatible with the subsequent use of a correlation for the length of the intermittent zone, which has a built-in assumption that the starting point is at zero intermittency.

The comparisons for flow TRB are presented next. It is seen from the skin-friction coefficient curves of Fig. 12 that all the transition criteria predict the start of transition far too early. The length of the calculated transition region is also too large. The determining factor for the correlations in this case is the streamwise pressure gradient. The boundary layer before transition was close to laminar separation and transitioned to a turbulent boundary layer in a very short distance. Presumably, in such a flow, upstream history effects, which the models do not incorporate, play an important role. Although by no means an unusual flow, this boundary layer appears to lie outside the bounds of the data that were used to develop the models and criteria for the transition calculation.

The final comparison is for flow TRC, which is more representative of turbomachinery conditions where turbulence levels are high and the pressure gradient is expected to play much less of a role in determining the onset of transition. Here, because of the high turbulence level, transition had set in before the first measurement location. However, the calculations were started at this point and all of the criteria predicted the onset of transition here. However, the determination of the extent of the transition zone still remains a problem. It is seen from Fig. 12 that the computed intermittency rises far too rapidly, resulting in too short a transition region.

In a recent paper, Narasimha et al.[29] show that especially near onset, the transition region is very sensitive to the applied pressure gradient and can be significantly asymmetric. They point out that assumptions of similarity [Eq. (3)] no longer hold and that models based on the spot formation rate such as those of Chen and Thyson must be modified to account for the effects of pressure gradient. The comparisons for TRB and TRC substantiate their findings that the transition under the influence of strong pressure gradients cannot be predicted properly by existing models.

Conclusions

The foregoing discussion of the modeling of surface roughness effects in boundary-layer flows has shown that it is, in principle, possible to model a variety of technically relevant, three-dimensional, stochastic roughnesses in terms of selected and directly measurable statistical parameters, the ratio λ/R_a, and the rms slope angle variation $\langle\alpha\rangle$. In this fashion, it is possible to get away from the need to determine the equivalent sand grain roughness for each different type of roughness. It is felt that the correlation developed herein is valid for a limited class of surfaces, such as certain types of turbomachinery blading. However, it must be stressed that for such a correlation to have more general applicability, further experiments on additional rough surfaces are needed to determine more accurately the trends with changes in the various roughness parameters.

The comparisons between data taken in a set of boundary layers undergoing laminar/turbulent transition, and the predictions of such boundary layers using models for transition that are currently in fairly wide use, point to various shortcomings of such models and suggest possible explanations for these failures. The criteria for determining the onset of transition used in the computations did not perform well. It appears that many additional factors present but not accounted for in engineering situations (such as upstream effects) play an important role in this process. The use of an intermittency distribution to determine the length of the transition region seems to be a reasonable approach in principle; however, this has to be coupled properly with the transition onset correlation and formulations of this intermittency distribution must account for the transverse variations within the transition region and also reflect the rather strong effects of the streamwise pressure gradient.

References

[1]Acharya, M., Bornstein, J., and Escudier, M.P., "Turbulent Boundary Layers on Rough Surfaces," *Experiments in Fluids*, Vol. 4, Jan. 1986, pp. 33-47.

[2]Acharya, M., "Pressure Gradient and Free-Stream Turbulence Effects on Boundary-Layer Transition," Brown Boveri Research Center, Baden, Switzerland, Rept. KLR 85-127C, Dec. 1985.

[3]Schlichting, H., "Experimentelle Untersuchungen zum Rauhigskeitproblem," *Ingenieur-Archiv*, Vol. 7, No. 1, Feb. 1936, pp. 1-34.

[4]Cebeci, T. and Chang, K.C., "Calculation of Incompressible Rough-Wall Boundary-Layer Flows," *AIAA Journal*, Vol. 16, July 1978, pp. 730-735.

[5]Betterman, D., "Contribution a l'Etude de la Convection Forcee Turbulente le Long de Plaques Rugueuses," *International Journal of Heat and Mass Transfer*, Vol. 9, Feb. 1966, pp. 153-164.

[6]Dvorak, F.A., "Calculation of Turbulent Boundary Layers on Rough Surfaces in Pressure Gradient," *AIAA Journal*, Vol. 7, Sept. 1969, pp. 1752-1759.

[7]Dirling, R.B., "A Method for Computing Rough Wall Heat Transfer Rates on Reentry Nosetips," AIAA Paper 73-763, 1973.

[8]Lewis, M.J., "An Elementary Analysis for Predicting the Momentum- and Heat-Transfer Characteristics of a Hydraulically Rough Surface," ASME Paper 75-HT-JJ, 1975.

[9]Finson, M.L., "A Model for Rough Wall Turbulent Heating and Skin Friction," AIAA Paper 82-0199, 1982.

[10]Lin, T.C. and Bywater, R.J., "Turbulence Models for High-Speed, Rough-Wall Boundary Layers," *AIAA Journal*, Vol. 20, March 1982, pp. 325-333.

[11]Turner, A.B., "Local Heat Transfer Measurements on a Gas Turbine Blade," *Journal of Mechanical Engineering Science*, Vol. 13, No. 1, 1971, pp. 1–12.

[12]Walker, G.J., "A Family of Surface Velocity Distributions for Axial Compressor Blading and Their Theoretical Performance," *Journal of Engineering for Power*, Vol. 98, April 1976, pp. 229-241.

[13]Graziani, R.A., Blair, M.F., Taylor, J.R., and Mayle, R.E., "An Experimental Study of Endwall and Airfoil Surface Heat Transfer in a Large Scale Turbine Blade Cascade," *Transactions of ASME, Journal of Engineering for Power*, Vol. 102, April 1980, pp. 257-267.

[14]Seyb, N.J., "The Role of Boundary Layers in Axial-Flow Turbomachines and the Prediction of Their Effects," AGARD AG164, Paper 14, Dec. 1972.

[15]Dunham, J., "Prediction of Boundary-Layer Transition on Turbomachinery Blades," AGARD AG164, Paper 3, Dec. 1972.

[16]McDonald, H. and Fish, R.W., "Practical Calculations of Transitional Boundary Layers," *International Journal of Heat and Mass Transfer*, Vol. 16, Sept. 1973, pp. 1729-1744.

[17]Forest, A.E., "Engineering Predictions of Transitional Boundary Layers," AGARD CP 224, May 1977.

[18]Abu-Ghannam, B.J. and Shaw, R., "Natural Transition of Boundary Layers—the Effects of Turbulence, Pressure Gradient and Flow History," *Journal of Mechanical Engineering Science*, Vol. 22, No. 5, 1980, pp. 213-228.

[19]Blair, M.F., "Influence of Free-Stream Turbulence on Boundary Layer Transition in Favorable Pressure Gradients," *Transactions of ASME, Journal of Engineering for Power*, Vol. 104, Oct. 1982, pp. 743-750.

[20]Acharya, M., Bornstein, J., Escudier, M.P., and Vokurka, V., "Development of a Floating Element for the Measurement of Surface Shear Stress," *AIAA Journal*, Vol. 23, March 1985, pp. 410-415.

[21]Patankar, S.V. and Spalding, D.B., *Heat and Mass Transfer in Boundary Layers*, Intertext Books, London, 1967.

[22]Crawford, M.E. and Kays, W.M., "STAN5—A Program for Numerical Computation of Two-Dimensional Internal and External Boundary-Layer Flows," NASA CR-2742, 1976.

[23]Cebeci, T. and Smith, A.M.O., *Analysis of Turbulent Boundary Layers*, Academic Press, New York, 1974.

[24]Jayatilleke, C.L.V., "The Influence of Prandtl Number and Surface Roughness on the Resistance of the Laminar Sublayer to Momentum and Heat Transfer," *Progress in Heat and Mass Transfer*, Vol. 1, 1969, pp. 193-329.

[25]Chen, K.K. and Thyson, N.A., "Extension of Emmons' Spot Theory to Flows on Blunt Bodies," *AIAA Journal*, Vol. 9, Sept. 1971, pp. 821-825.

[26]Emmons, H.W., "The Laminar-Turbulent Transition in a Boundary Layer—Pt. 1," *Journal of the Aeronautical Sciences*, Vol. 18, July 1951, pp. 490-498.

[27]Dhawan, S. and Narasimha, R., "Some Properties of Boundary Layer Flow During the Transition From Laminar to Turbulent Motion," *Journal of Fluid Mechanics*, Vol. 3, Pt. 4, Jan. 1958, pp. 418-436.

[28]Morkovin, M.V., "Instability, Transition to Turbulence and Predictability," AGARDograph 236, July 1978.

[29]Narasimha, R., Devasia, K.J., Gururani, G., and Badri Narayanan, M.A., "Transitional Intermittency in Boundary Layers Subjected to Pressure Gradient," *Experiments in Fluids*, Vol. 2, No. 4, Nov. 1984, pp. 171-176.